RESEARCH ARTICLE

Development of mix design method based on statistical analysis of different factors for geopolymer concrete

Paramveer SINGH, Kanish KAPOOR[*]

Department of Civil Engineering, Dr B R Ambedkar National Institute of Technology, Jalandhar 144011, India
[*]*Corresponding author. E-mail: kapoork@nitj.ac.in*

ABSTRACT   The present study proposes the mix design method of Fly Ash (FA) based geopolymer concrete using Response Surface Methodology (RSM). In this method, different factors, including binder content, alkali/binder ratio, NS/NH ratio (sodium silicate/sodium hydroxide), NH molarity, and water/solids ratio were considered for the mix design of geopolymer concrete. The 2D contour plots were used to setup the mix design method to achieve the target compressive strength. The proposed mix design method of geopolymer concrete is divided into three categories based on curing regime, specifically one ambient curing (25 °C) and two heat curing (60 and 90 °C). The proposed mix design method of geopolymer concrete was validated through experimentation of M30, M50, and M70 concrete mixes at all curing regimes. The observed experimental compressive strength results validate the mix design method by more than 90% of their target strength. Furthermore, the current study concluded that the required compressive strength can be achieved by varying any factor in the mix design. In addition, the factor analysis revealed that the NS/NH ratio significantly affects the compressive strength of geopolymer concrete.

KEYWORDS   geopolymer concrete, mix design, fly ash, response surface methodology, compressive strength, stress−strain

1   Introduction

Concrete is the leading construction material of infrastructure development and its consumption is increasing day by day with the rapid growth of infrastructural activities globally. As a result, this increases the consumption of Portland Cement (PC), a primary binder used for concrete production. It is well known that PC is responsible for 75%–80% of the total CO_2 emissions of a concrete mix [1]. In addition, the cement industry contributes about 5%–7% by weight of global CO_2 emissions [2]. Therefore, extensive research has been conducted internationally to determine alternatives for PC concrete to minimize CO_2 emissions. In line with this, geopolymer concrete seems to be an unparalleled substitute for PC concrete that reduces CO_2 emissions by 75%–90% and promotes sustainable development [3]. Geopolymer concrete is an innovative concrete that consists of binder rich in Silica (Si), Alumina (Al), alkali activators, and aggregates. The binders used in geopolymer concrete react with alkaline activators, forming a polymer chain network as the final product. Many binders, such as Fly Ash (FA), Ground Granulated Blast Furnace Slag (GGBS), and Rice Husk Ash (RHA) Metakaolin (MK) are used in geopolymer concrete at different stages. However, the use of FA and GGBS as binders was found to be most judicious since they eliminate the problem of dumping or land filling their waste products. Moreover, FA and GGBS are both rich in Si and Al, which aids in the production of geopolymer concrete [4,5]. Sodium hydroxide (NH) and sodium silicate (NS) activators are typically used in geopolymer concrete to dissolute the Si and Al of the binder and form a tetrahedral aluminosilicate polymeric chain. Geopolymer concrete possesses excellent properties, specifically high strength, low creep and shrinkage, good resistance to fire, acids, and sulfate attacks [6]. These properties depend on various factors, such as type of binder, binder content and properties, quantity of alkali activators, hydroxide concentration, additional water, and curing regime. These factors can

individually or collectively influence the final properties of geopolymer concrete to a large extent. Bernal et al. [7] used varying binder contents to evaluate the compressive strength of concrete and concluded that strength increases with the increase of binder content in concrete. Hardjito et al. [8] concluded that the molarity of NH, water/solid ratio, and curing regime affect the compressive strength of geopolymer concrete. An increase in water/solid ratio decreases the compressive strength whereas an increase in curing temperature escalates the compressive strength. Verma and Dev [9] used different molarities of NH (8 to 16 mol·L^{-1}) and varying NS/NH ratios (0.5 to 3) to evaluate the mechanical properties of FA-based geopolymer concrete. Their results show that 14 M NH with a NS/NH ratio of 2.5 was optimal for geopolymer concrete. Noushini and Castel [10] used different heat curing temperatures (i.e., 60, 75, and 90 °C) and ambient curing to evaluate the properties of geopolymer concrete and found that 75 °C heat curing is optimal for compressive strength. These previous studies have showed that there are no fixed criteria to attain the required strength. Rather, it can be achieved by varying different factors of the mix design of geopolymer concrete.

The low calcium (Class-F) FA was unable to provide the required strength with ambient curing, thus heat curing is required to increase the strength [11,12]. Heat curing is also a key issue at sites to obtain the desired results. To overcome this issue, high calcium mineral is used in Class-F FA based geopolymer concrete. GGBS is mostly used with Class-F FA to accelerate the chemical reaction between the binder and alkali solution for geopolymer concrete at ambient curing. The Class-F FA can provide the appropriate strength with the addition of GGBS in geopolymer concrete at ambient curing. Mallikarjuna Rao and Gunneswara Rao [13] used GGBS as a partial replacement of FA and obtained optimum compressive strength at 50% replacement of FA with GGBS. Nath and Sarker [14] used ambient curing temperature and attained 55 MPa strength with 30% GGBS incorporation with FA. Nagajothi and Elavelin [15] revealed that compressive strength increased up to 40% with the addition of 30% GGBS at ambient curing. The addition of GGBS during geopolymer concrete preparation produces calcium silicate gel along with polymeric chain of Si and Al, which consequently enhances the compressive strength of the concrete. With the above in mind, the addition of GGBS during geopolymer concrete preparation at ambient curing is beneficial in the case of a high strength requirement and should give promising results.

Researchers have proposed various mix designs of geopolymer concrete based on their experimental results obtained using a trial-and-error approach and fixed design factors. In conformity with pre-existing studies, the mix design for geopolymer concrete is generally proposed based on target strength, performance-based mix design,

and software-based model. Li et al. [16] proposed a mix design with a fixed alkali dosage and varying binder content, alkali activator composition, and water content to attain the required strength. Similarly, Pavithra et al. [17] proposed a mix based on target strength, in which NH molarity is fixed at 16 mol·L^{-1} and NS/NH ratio at 1.5 for all mixes with a varying dosage of total alkali content. Patankar et al. [18] also kept the majority of the mix factors constant, with the exception of binder content and fineness of FA for the mix design of geopolymer concrete. Further, Ferdous et al. [19], Anuradha et al. [20], and Talha Junaid et al. [21] fixed the binder content for their proposed mix design and varied the content of other factors to achieve their desired target strength. Luan et al. [22] proposed a mix design method based on target strength and workability by varying different factors that effect the compressive strength of geopolymer concrete. Their results concluded that the NS/NH ratio and NH concentration are the main factors affecting the compressive strength of concrete. A performance-based mix design was proposed by Bondar et al. [23] based on the effect of chloride and binding properties of geopolymer concrete. Furthermore, Hadi et al. [24] and Karthik and Mohan [25] proposed a mix design with varying geopolymer concrete parameters using the Taguchi method. Riahi et al. [26] and Olivia and Nikraz [27] also used the Taguchi method with varying geopolymer concrete parameters at different curing temperatures. Lokuge et al. [28] used the Multivariate Adaptive Regression Spline (MARS) model to determine a statistical relationship between alkali/binder (Al/binder) ratio, NH molarity, NS/NH ratio, and water/geopolymer solids ratio and attain the required strength of geopolymer concrete. Gunasekara et al. [29] proposed a mix design using artificial neural network with varying Al/binder ratio, NH molarity, NS/NH ratio, and water/geopolymer solids ratio to obtain the target compressive strength within the range of 25–45 MPa. In addition to the mix design method, identifying the influence of each factor on the final result is also a key aspect. Vu-Bac et al. [30] used sensitivity analysis to predict the most and least significant factor for their output results. Similarly, other researchers also used different techniques to predict the influence of each factor on their output results [31–34]. Vu-Bac et al. [35] used multiscale modeling for polymer nanocomposites to evaluate the factor impact on output results.

Based on previous research, the present study identified a range of factors for the proposed mix design, specifically the binder content, Al/binder ratio, NH molarity, NS/NH ratio, and water/solid ratio. The Response Surface Methodology (RSM) was used to establish the relationship between different factors required for the proposed mix design to achieve the required compressive strength.

2 Research significance

As seen from the literature discussed above, the available mix designs of geopolymer concrete are mostly based on either a fixed binder content or alkali/binder ratio for a single curing regime. Additionally, few mix designs of geopolymer concrete are based on trial-and-error or partially fixed factors. To date, existing mix designs are limited by the fixed factors of geopolymer concrete mix designs. Limited research has been conducted to develop a standard mix design for geopolymer concrete with varying factors to achieve the target compressive strength. Furthermore, no studies have been carried out to determine a way to attain the target compressive strength with different curing regimes and varying factors. In this study, different factors, such as binder content, Al/binder ratio, NH molarity, NS/NH ratio, water/solid ratio, and curing regime were varied for the mix design of geopolymer concrete. Primarily, RSM was used to develop the mix design method of geopolymer concrete with varying factors, especially the curing regime. The proposed mix design was then divided into three categories based on the curing regime, such as one ambient curing (25 °C) and two heat curing (60 and 90 °C). Each category of the curing regime consists of statistical relation between different factors in the form of 2D contour plots (i.e., binder content, Al/binder ratio, NH molarity, NS/NH ratio and water/solids ratio) to attain the target compressive strength. Each curing regime was further divided into subcategories based on the required strength (i.e., 20, 30, and 40 MPa, and 50, 60, and 70 MPa). The different factors for mix proportioning, specifically M30, M50, and M70, for all curing regimes were selected from 2D contour plots and experimentally evaluated in terms of compressive strength at 7 and 28 d of curing.

3 Proposed mix design procedure

3.1 Mix design database

In this study, the mix design of geopolymer concrete incorporating Class-F FA and GGBS was designed based on existing literature. The collected data include the binder content, Al/binder ratio, NH molarity, NS/NH ratio, water/solids ratio, and curing regime, which were mainly collected on the basis of the primary binder, i.e., Class-F FA with incorporation of GGBS. The data was also used for RSM modeling.

3.2 Response surface methodology model

The RSM model was first introduced by Box and Wilson in 1950 [36]. RSM considers the interaction between input variables and one or more output parameters. It is a beneficial method to estimate the precise model with a small amount of experimental data [37], though it is more useful when output is dependent on multiple variables [38]. The RSM examines an appropriate relationship between the input and output variables to identify the optimal operating conditions for a system under study. Box-Behnken Design (BBD), Central Composite Design (CCD), and Optimal Design are the main experimental designs used in RSM [39]. The experimental data are evaluated to fit a statistical model, such as linear, quadratic, cubic or 2FI (two factor interaction). The model factors are denoted in the form of A, B, C, and so on for linear independent variables. Similarly, the factors for the two factor and quadratic models are denoted as AB, BC, CA and A^2, B^2, C^2, and so on, respectively. The model adequacies used are by determination coefficient (R^2), adjusted determination coefficient (Adj-R^2), and adequate precision. Moreover, lack of fit is also determined to check the adequacy of the model. Differences between means were tested for statistical significance using Analysis of Variance (ANOVA) [40].

The algorithm of the RSM model is generally based on input variable, or factors, and output dependent variable. The exact relation between the input and output variables depends on the fitted model and their adequacy. The general equation denoting the relationship between the input and output variables of the RSM model is:

$$Y = f(x_n) + e,$$

$$x_n \text{ denotes to } x_1, x_2, x_3 ... \text{ up to } x_n,$$

where Y is the dependent output variable, $f(x_n)$ is a function of the input independent variables, n is the number of independent variables, and e is the regression error. The RSM is used by many researchers for screening and optimization. The methodology utilized in this study is shown in Fig. 1. The application of the model includes problem identification, determination of input and output variables, selection of factors, analysis design and evaluation. Finally, the model is validated through experimentation.

3.3 Response surface methodology model development and evaluation

In this study, the optimal RSM is used to establish a model based on factors, such as binder content, Al/binder ratio, NH molarity, NS/NH ratio, water/solids ratio and curing regime. The ranges of each factor used for the statistical model are given in Table 1. The ranges of each factor were decided based on the literature database provided as a supplementary material, which included 175 data points. The stepwise procedure from problem identification, determination of input and output variables, model analysis and validation of study is given
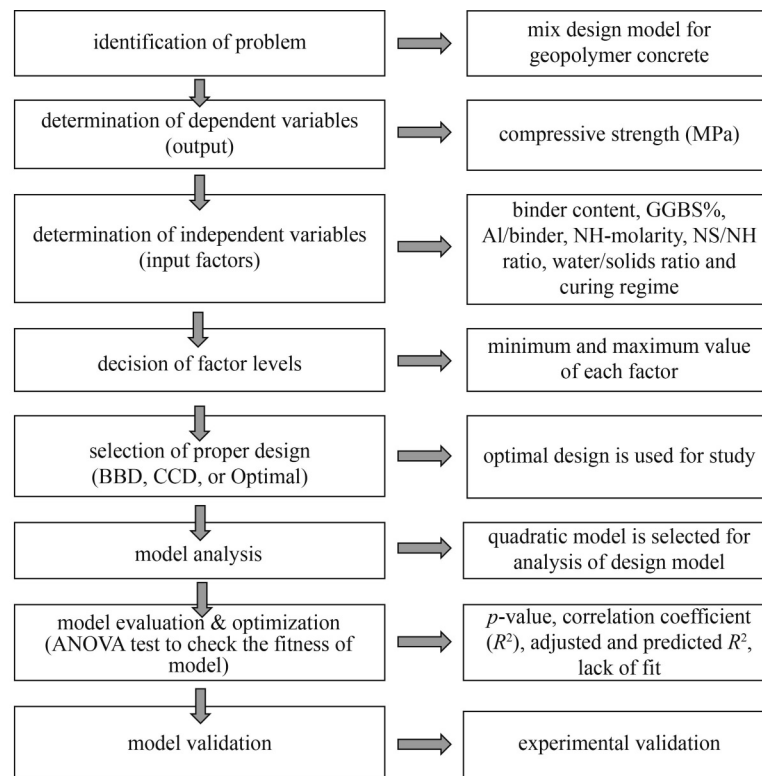
Fig. 1 The entire procedure of response surface methodology (RSM) of present study.

Table 1 Factor ranges used in the study for mix proportioning of geopolymer concrete

factor	name	unit	minimum	maximum	average	standard deviation
A	binder content	$kg·m^{-3}$	300	500	403.58	46.62
B	GGBS	$\%$	0	40	14.71	18.92
C	Al/binder	−	0.35	0.65	0.44	0.095
D	NS/NH	−	1.50	3.50	2.36	0.37
E	NH	$mol·L^{-1}$	8	16	11.18	2.83
F	water/solids	−	0.15	0.30	0.23	0.04
G	temperature	°C	25	100	58.43	23.12

in Fig. 1. Firstly, problem identification of the current study is to develop the mix design of geopolymer concrete. Secondly, compressive strength is considered as the output variables, which depend on the selected factors, or input variables, specifically binder content, Al/binder ratio, NH molarity, NS/NH ratio, water/solids ratio, and curing regime. Thirdly, the ranges of each factor were decided based on literature data and required output from the analysis. The RSM model for this study was selected for analysis since multiple factors affect the output variable. After that, model analysis was conducted and a quadratic model was suggested based on the R^2 value as shown in Table 2.

The fitness of model of the suggested model was checked using ANOVA test as shown in Table 3. The results show good fit for the model with a statistically significant p-value (< 0.05) and insignificant lack of fit

(> 0.05) with a mean square of 1594.89. The model F-value of 40.01 implies the model is significant with only a 0.01% chance that an F-value this large would occur due to noise. The p-values less than 0.05 indicate model terms and their relation with each other are all significant. The lack of fit F-value of 1.13 implies the lack of fit is not significant relative to the pure error. There is a 34.63% chance that a lack of fit F-value this large could occur due to noise. The insignificant lack of fit is good for acceptance of the model. Furthermore, the model statistics, including the R^2 value, standard deviation, and adequate precision are shown in Table 4. The difference between the adjusted and predicted R^2 is less than 0.2, which shows reasonable agreement to fit the model. The standard deviation of the output results is 6.31, which is also satisfactory for the model. Moreover, an adequate precision value of 31 shows good fitness of model since it

Table 2 Initial summary of different statistical model

source	sequential p-value	lack of fit p-value	R^2	adjusted R^2	predicted R^2	remarks
linear	< 0.0001	< 0.0001	0.42	0.40	0.36	–
2FI	< 0.0001	0.20	0.84	0.81	0.78	–
quadratic	0.040	0.27	0.85	0.82	0.79	suggested
cubic	0.01	0.85	0.94	0.87	–	aliased

Table 3 ANOVA test results for input variables for output results

source	sum of squares	df	mean square	F-value	p-value	remarks
model	35087.59	22	1594.89	40.01	< 0.0001	significant
A-Binder content	198.16	1	198.16	4.97	0.0272	
B-GGBS %	1484.49	1	1484.49	37.24	< 0.0001	
C-Al/binder	499.67	1	499.67	12.53	0.0005	
D-NS/NH	2586.99	1	2586.99	64.90	< 0.0001	
E-NH	277.97	1	277.97	6.97	0.0091	
F-water/solids	1952.08	1	1952.08	48.97	< 0.0001	
G-Temperature	719.37	1	719.37	18.05	< 0.0001	
AC	823.01	1	823.01	20.65	< 0.0001	
AD	658.84	1	658.84	16.53	< 0.0001	
AE	879.06	1	879.06	22.05	< 0.0001	
AF	298.37	1	298.37	7.49	0.0070	
BC	155.51	1	155.51	3.90	0.0501	
BD	1995.49	1	1995.49	50.06	< 0.0001	
BF	132.81	1	132.81	3.33	0.0699	
BG	286.15	1	286.15	7.18	0.0082	
CD	182.36	1	182.36	4.57	0.0340	
CE	4586.99	1	4586.99	115.07	< 0.0001	
DF	2058.58	1	2058.58	51.64	< 0.0001	
EF	2565.47	1	2565.47	64.36	< 0.0001	
B^2	183.07	1	183.07	4.59	0.0337	
C^2	226.36	1	226.36	5.68	0.0184	
G^2	600.03	1	600.03	15.05	0.0002	
residual	6058.98	152	39.86	–	–	
lack of fit	4791.46	117	40.95	1.13	0.3463	not significant
pure error	1267.51	35	36.21	–	–	
cor total	41146.57	174	–	–	–	

Table 4 Model performance statistics

source	R^2	adjusted R^2	predicted R^2	standard deviation
quadratic model	0.85	0.83	0.81	6.31

is greater than 4 [41]. Therefore, overall performance of the model shows a significant relation between the input and output variables based on ANOVA and model statistics performance. Furthermore, Fig. 2 shows the predicted and actual compressive strength. The data points and trend line show little deviation, which in result validates the model.

3.4 Effect of factors on compressive strength using response surface methodology model

The mix design is divided based on different curing temperatures, i.e., one ambient curing (25 °C) and two heat curing (60 and 90 ºC). The 2D contour plots of each curing category are divided into two subcategories based

on strength, i.e., 20–40 MPa and 50–70 MPa. Each strength subcategory contains four contour plots i.e., binder content vs Al/binder ratio, Al/binder ratio vs NH molarity, NH molarity vs NS/NH ratio, and NH molarity vs water/solid ratio, as shown in Figs. 3–8. The contour

plots are used to produce the mix proportioning of geopolymer concrete for the required compressive strength at 28 d of curing for a 100 mm cube. Every factor used in the mix design has a different effect on the compressive strength of geopolymer concrete as discussed below.

3.4.1 Binder content

In the mix design, Class-F FA has been proposed as a precursor binder and GGBS has been used as a FA replacement of within 0% to 40% to attain the target strength. The FA content ranges from 420 to 500 kg·m^{-3}. The ANOVA test results presented in Table 3 show a p-value greater than 0.05 for the binder content, making it statistically insignificant and less impactful compared to the other factors. However, it is still necessary to select a range for the binder content of the geopolymer concrete
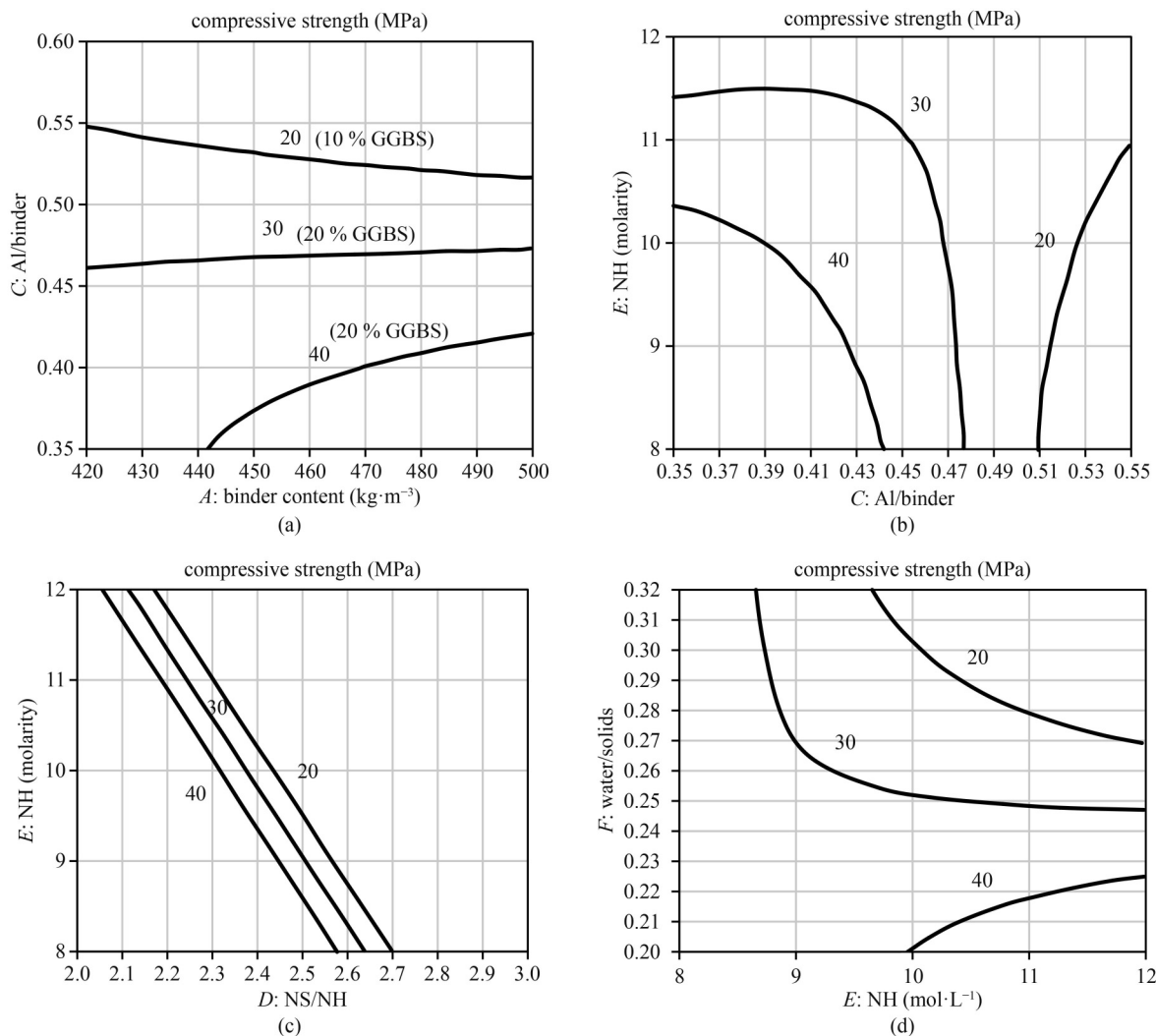
Fig. 2 Predicted and actual compressive strength in (MPa) of the adopted model

Fig. 3 The 2D contour plots for 20, 30, and 40 MPa at ambient curing −25 °C: (a) binder content vs Al/binder ratio; (b) Al/binder ratio vs NH molarity; (c) NH molarity vs NS/NH; (d) NH molarity vs water/solids ratio.

Fig. 4   The 2D contour plots for 50, 60, and 70 MPa at ambient curing −25 °C: (a) binder content vs Al/binder ratio; (b) Al/binder ratio vs NH molarity; (c) NH molarity vs NS/NH; (d) NH molarity vs water/solids ratio.
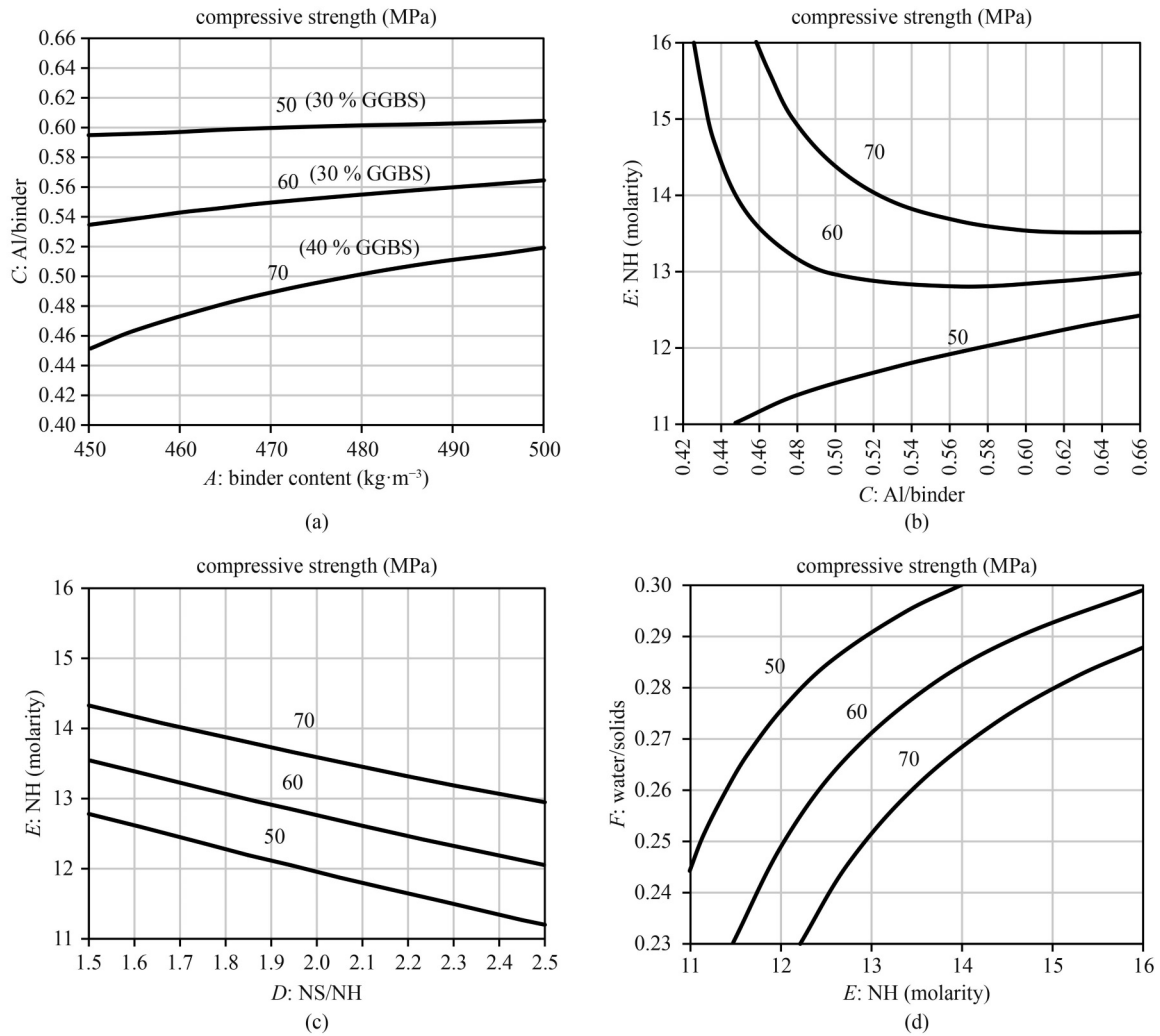
as per requirement. For a 20–40 MPa target strength, the minimum binder content is 420 kg·m^{-3} and the maximum is 500 kg·m^{-3} for all curing conditions. Similarly, for a 50–70 MPa strength range, the minimum binder content is 450 kg·m^{-3} and the maximum is 500 kg·m^{-3}.

Moreover, the GGBS used as an FA replacement will vary depending on the required compressive strength. For the ambient curing condition, a 20–40 MPa target compressive strength is required up to 20% GGBS (Fig. 3(a)). whereas for a 50–70 MPa target compressive strength, the GGBS content increases up to 40% (Fig. 4(a)). This shows that a higher GGBS content is required for the ambient curing condition to achieve a higher compressive strength. For the 60 and 90 °C curing conditions, the GGBS content is reduced to 10% for a 20–40 MPa target compressive strength (Figs. 5(a) and 7(a)). For a 50–60 MPa target strength, the GGBS content is reduced to 30% and 20% for 60 and 90 °C curing, respectively (Figs. 6(a) and 8(a)). This shows that heat curing reduces GGBS consumption in geopolymer

concrete when attaining the required compressive strength.

3.4.2   Alkali/binder ratio

The Al/binder ratio, i.e., the weight ratio of alkali activators to total binder content is used in the mix design of geopolymer concrete. The Al/binder ratio used in the mix design is a combination of NH and NS to achieve the desired results. The Al/binder ratio ranges between 0.35 and 0.65 for all mix designs of geopolymer concrete. The Al/binder ratio has a p-value of 0.0005, suggesting it significantly affects the compressive strength of concrete, as shown in Table 3. For ambient curing and a 20–40 MPa compressive strength, the Al/binder ratio varies between 0.35 and 0.55, as shown in Fig. 3(a). For a 50–70 MPa compressive strength, the ratio ranges between 0.45 and 0.6, as shown in Fig. 4(a). Furthermore, the Al/binder ratio for 60 °C curing ranges from 0.39 to 0.53 for a 20–40 MPa strength (Fig. 5(a)) and from 0.48 to
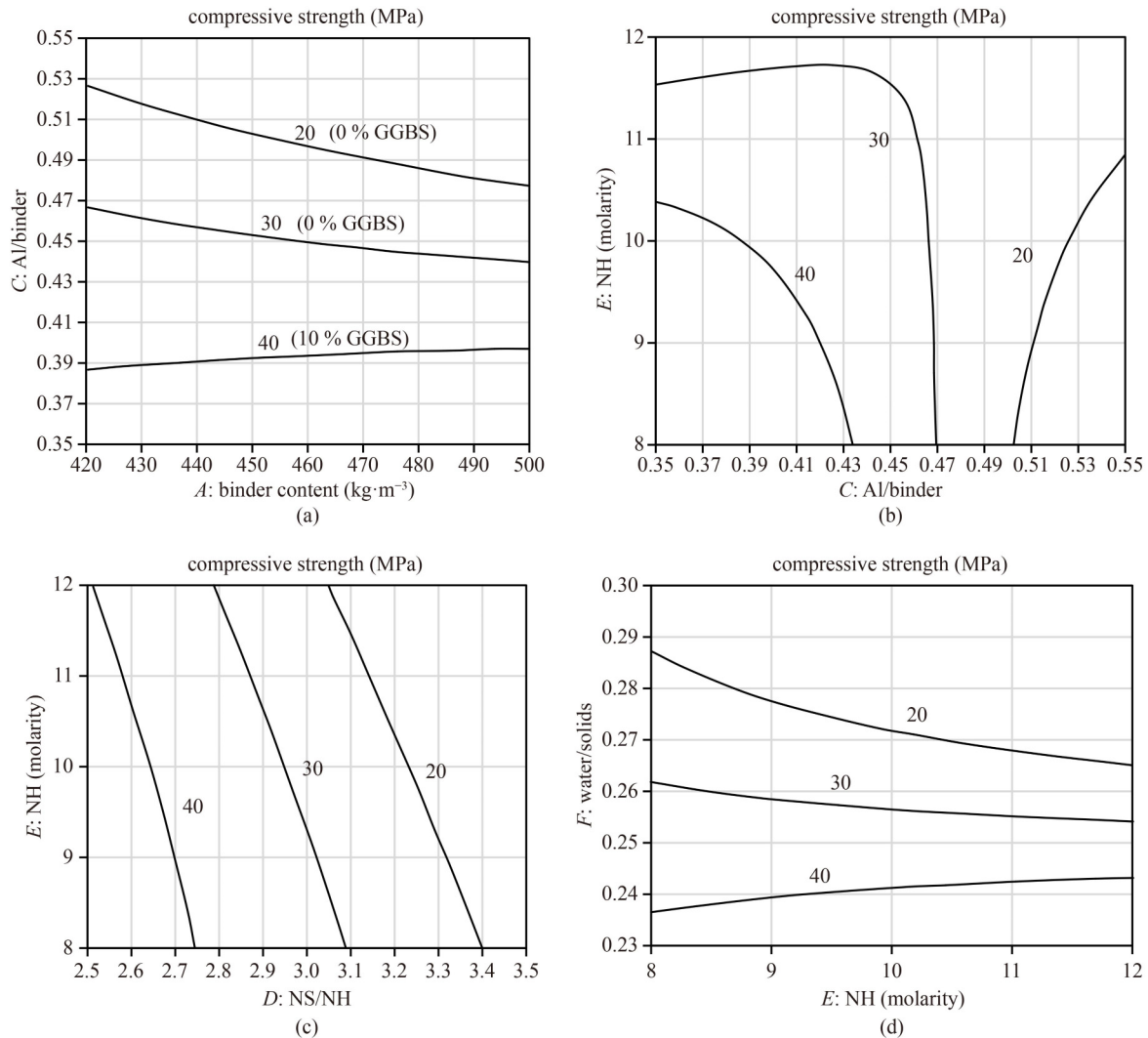
Fig. 5 The 2D contour plots for 20, 30, and 40 MPa at heat curing −60 °C: (a) binder content vs Al/binder ratio; (b) Al/binder ratio vs NH molarity; (c) NH molarity vs NS/NH; (d) NH molarity vs water/solids ratio.

0.58 for a 50–60 MPa target strength (Fig. 6(a)). For 90 °C curing, the Al/binder ratio ranges between 0.42 and 0.56 for 20–40 MPa and 0.5–0.58 for a 50–70 MPa target compressive strength, as shown in Figs. 7(a) and 8(a), respectively. This shows that a high value of Al/binder ratio is required for a higher compressive strength for all curing conditions.

3.4.3 Sodium hydroxide molarity

NH combined with NS has been used as an activator in the mix design of geopolymer concrete. The NH contents have been selected based on their molarity ($mol \cdot L^{-1}$) in the mix design of geopolymer concrete. In this mix design, the molarity ranges from 8 to 16 $mol \cdot L^{-1}$, which was selected based on previous studies. For all curing conditions, the NH molarity ranges between 8 and 12 $mol \cdot L^{-1}$ for a 20–40 MPa compressive strength and between 12 to 16 $mol \cdot L^{-1}$ for a 50–70 MPa strength, as

shown in Fig. 3–8(c). The p-value of 0.0091 suggests that the NH molarity is less significant than the Al/binder ratio for the target compressive strength of geopolymer concrete.

3.4.4 Sodium silicate/sodium hydroxide ratio

The NS content has been selected based on the NS/NH and Al/binder ratio. A NS/NH ratio between 1.5 and 3.5 was used in the mix design of geopolymer concrete. The p-value less than 0.0001 shows a much higher statistical significance of NS/NH ratio when achieving the required compressive strength. For all curing conditions, the NS/NH ratio mainly depends on the NH molarity, i.e., higher the NH molarity, lower the NS/NH ratio. The NS/NH ratio ranges from 2 to 3 for 20–40 MPa and from 1.5 to 2.5 for a 50–70 MPa target compressive strength of geopolymer concrete for all curing conditions, as shown in Fig. 3–8(c). A lower NS/NH ratio value gives a higher compressive strength and vice versa [42].
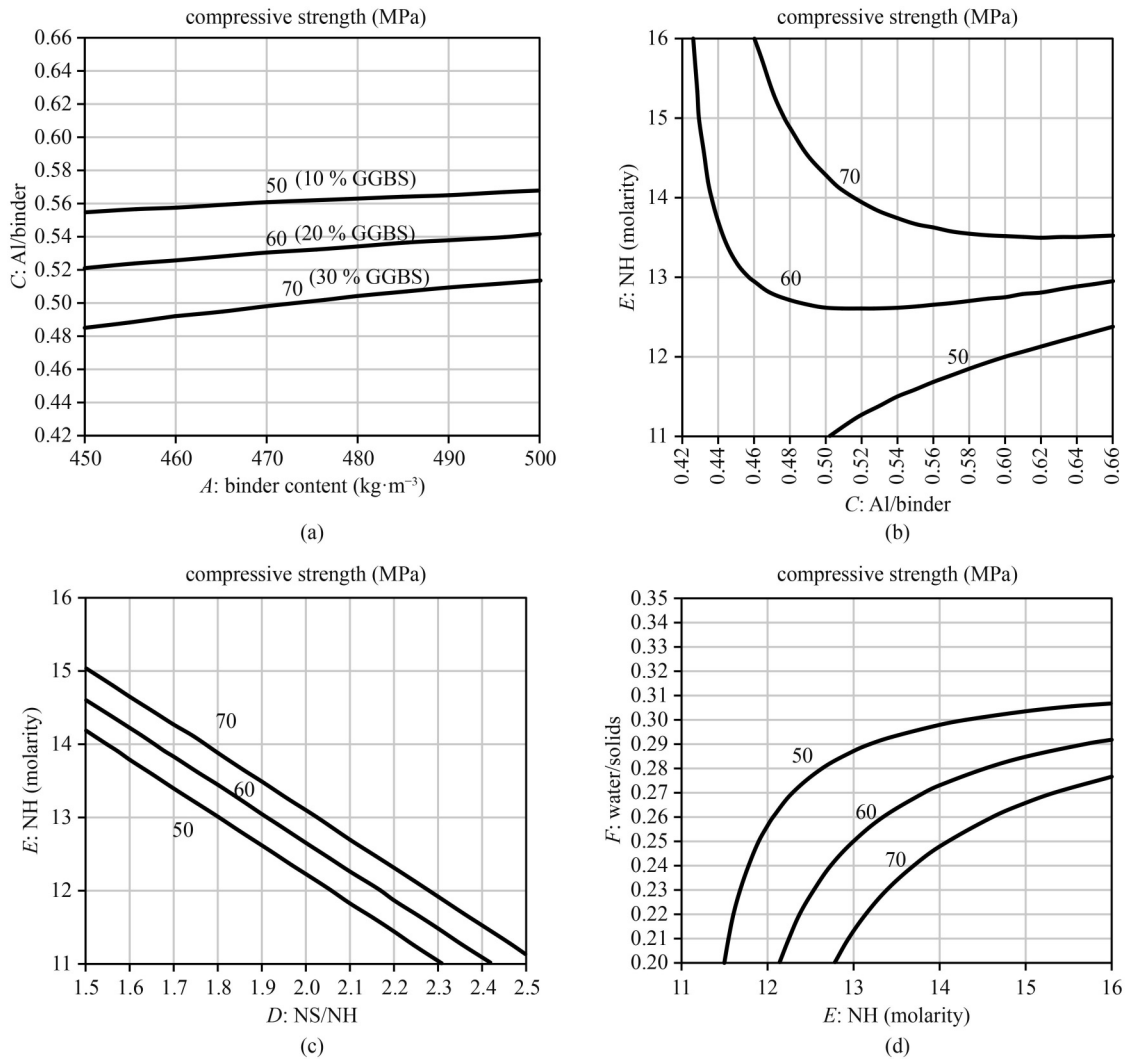
Fig. 6 The 2D contour plots for 50, 60, and 70 MPa at heat curing −60 °C: (a) binder content vs Al/binder ratio; (b) Al/binder ratio vs NH molarity; (c) NH molarity vs NS/NH; (d) NH molarity vs water/solids ratio.

3.4.5   Water/solid ratio

The water/solid ratio is the ratio of water, which includes the water content in NH, NS, and additional water present in geopolymer concrete, to the solids, which includes the solid content of NS, NH, and binder content. The water/solid ratio within the range of 0.15 to 0.35 was used in the mix design, which depends on the NH, NS, and binder content, as seen in Figs. 3–8(d). The water/solid ratio plays a significant role when acquiring the target compressive strength. A higher water/solid ratio results in a lower compressive strength and vice versa [43]. The p-value less than 0.0001 shows that the water/solid ratio has a significant effect on the output of compressive strength.

3.4.6   Aggregates

The quantity of aggregates for the mix design of geopolymer concrete depends on the Al/binder ratio and

was calculated in this study using a volumetric approach as per IS 10262:2019 [44]. The coarse aggregates with a maximum size of 12.5 mm and fine aggregates less than 4.75 mm were used for the mix design of geopolymer concrete.

4   Experiment validation of mix design

A compressive strength of 30, 50, and 70 MPa were assessed experimentally for each curing regime using 2D contour plots established through RSM model.

4.1   Material used

Class-F FA, obtained from the Nabha Power Limited Thermal Plant situated in Punjab, India, was used as a primary binder for the production of geopolymer concrete conforming to IS 3812 [45]. The GGBS was obtained
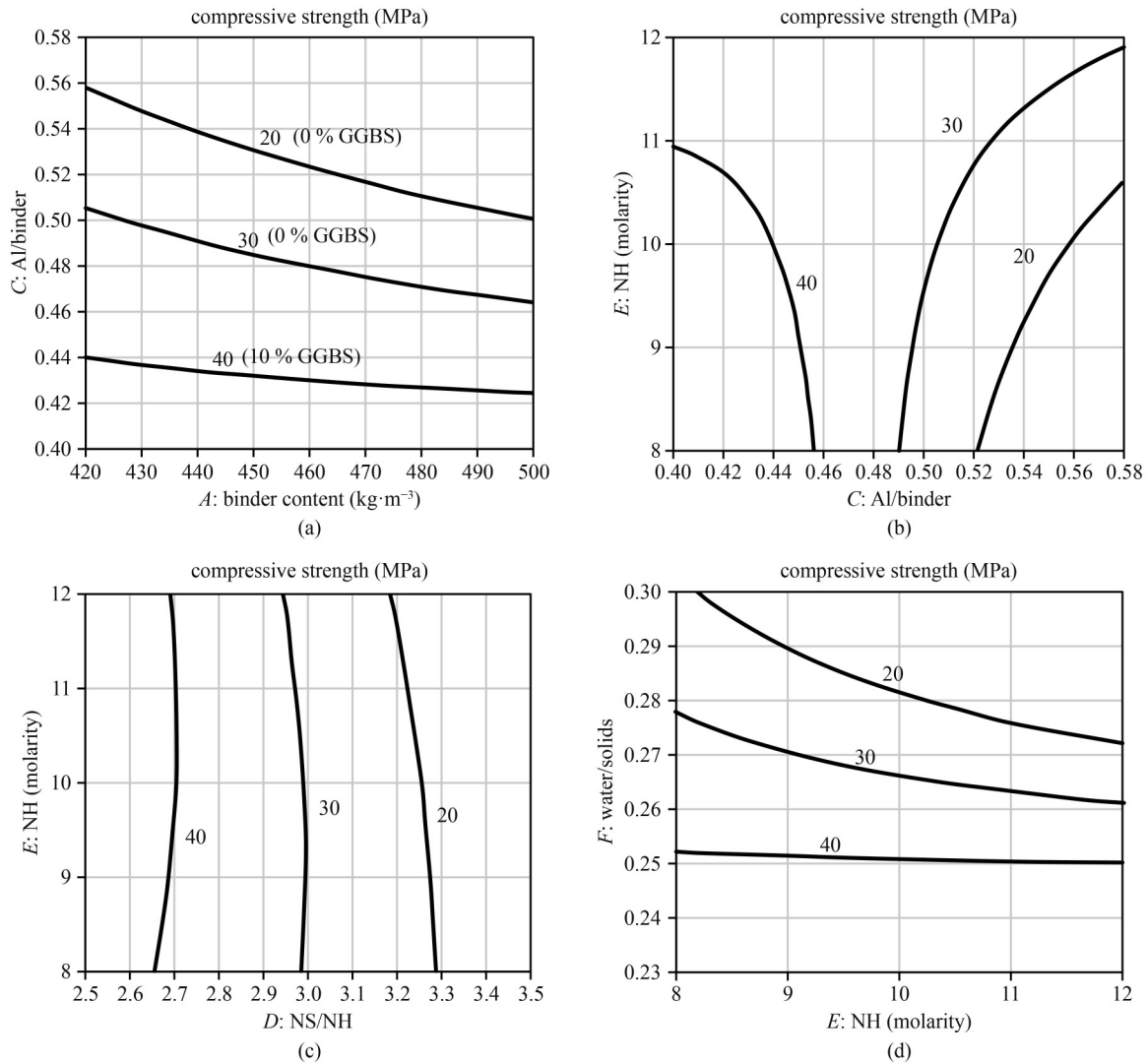
Fig. 7 The 2D contour plots for 20, 30, and 40 MPa at heat curing −90 °C: (a) binder content vs Al/binder ratio; (b) Al/binder ratio vs NH molarity; (c) NH molarity vs NS/NH; (d) NH molarity vs water/solids ratio.

from Aastra Chemicals located in Chennai, India conforming to BS:6699 and used a partial replacement of FA within the range of 0% to 40% as per requirement. The chemical and physical properties of FA and GGBS are tabulated in Tables 5 and 6. respectively. The commercially available NH and NS were used as alkaline activators in the preparation of geopolymer concrete. The NH was 98% pure in the form of solid pellets and mixed with water 24 hours prior to casting to obtain the desired concentration. The NS was in liquid form (composition: Na_2O = 14.7%, SiO_2 = 29.4% and 55.9% of H_2O by mass) with a specific gravity of 1.53. The coarse aggregates of maximum size of 12.5 mm and fine aggregates of size less than 4.75 mm are used conforming to IS 383:2016 [46]. The particle size distribution of the coarse and fine aggregates is given in Fig. 9. The coarse and fine aggregates had a specific gravity of 2.61 and 2.53, and water absorption of 0.5% and 1.5%, respectively.

4.2 Example of procedure and calculation for M30 geopolymer concrete for ambient curing

The input variables (factors) were selected from the proposed contour plots for required strength based on curing regime. For M30 concrete, the procedure and calculations are given below.

Step 1: Binder content vs Al/Binder ratio

In the first step of the mix design, the binder content or Al/binder is fixed to select the best combination to achieve the desired compressive strength using the given contour plots, as shown in Fig. 3(a)–3(d). Figure 3(a) contains the binder content (FA + GGBS) on the X axis ranging from 420 to 500 kg·m^{-3} Similarly, the Y axis contains the Al/binder ratio in the range of 0.35 to 0.55. For example, for a 30 MPa target strength, adopting a 420 kg·m^{-3} FA binder content with 20% GGBS will result in a 0.46 Al/binder ratio, as seen from the contour plot in Fig. 3(a).

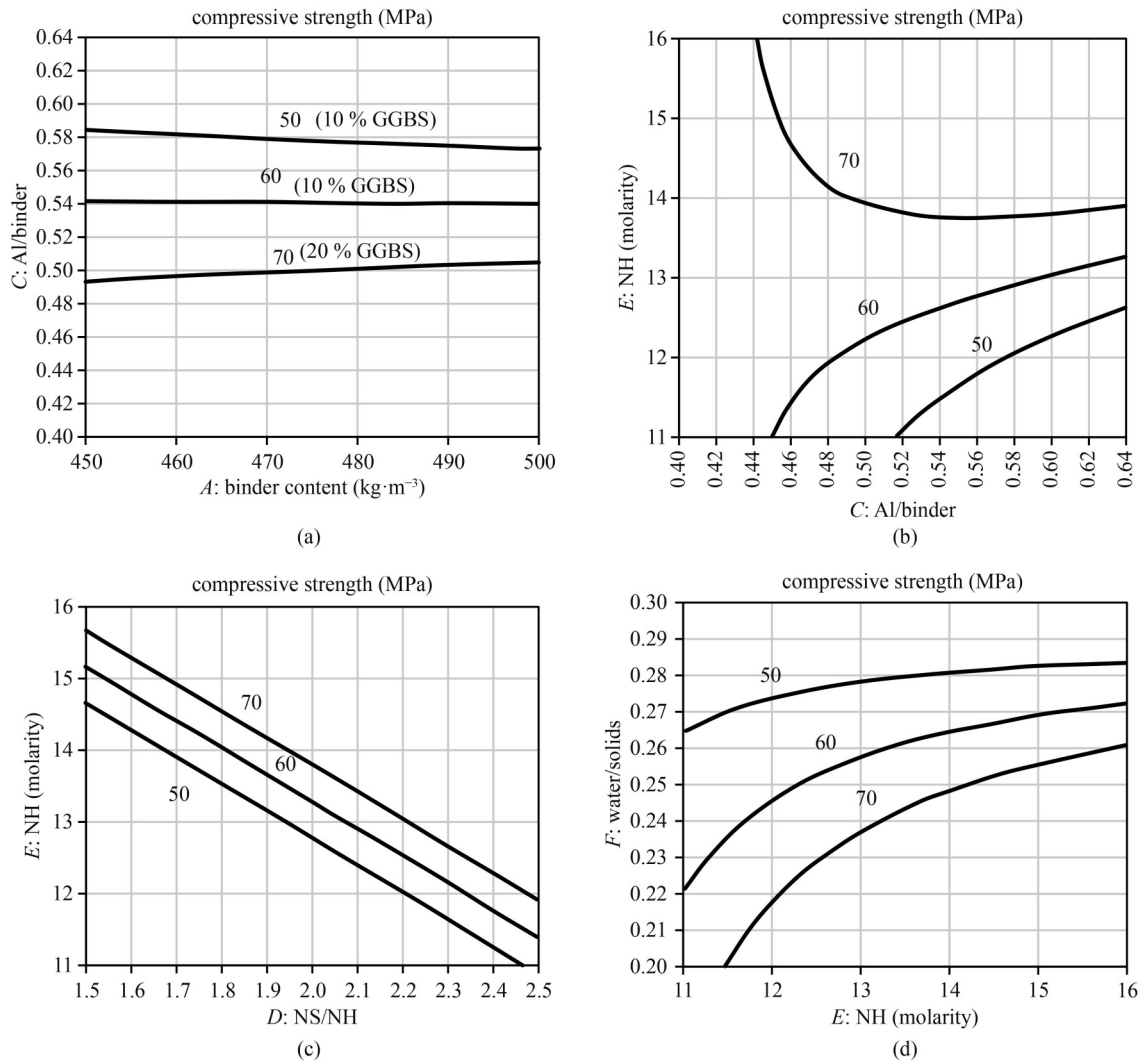Fig. 8 The 2D contour plots for 50, 60, and 70 MPa at heat curing −90 °C: (a) binder content vs Al/binder ratio; (b) Al/binder ratio vs NH molarity; (c) NH molarity vs NS/NH; (d) NH molarity vs water/solids ratio.

Table 5 Chemical properties of FA and GGBS

chemical compounds	FA	GGBS
SiO_2	54.5%	33.1%
Al_2O_3	33.9%	18.2%
Fe_2O_3	4.2%	0.31%
CaO	3.1%	35.3%
MgO	2.3%	7.6%
loss of ignition	1.3%	0.26%

Table 6 Physical properties of FA and GGBS

property	FA	GGBS
specific gravity	2.2	2.85
fineness (m^2/kg)	4025	3900

Fig. 9 Particle distribution of coarse and fine aggregates used in the study.

Step 2: Al/binder ratio vs NH molarity (mol·L^{-1})

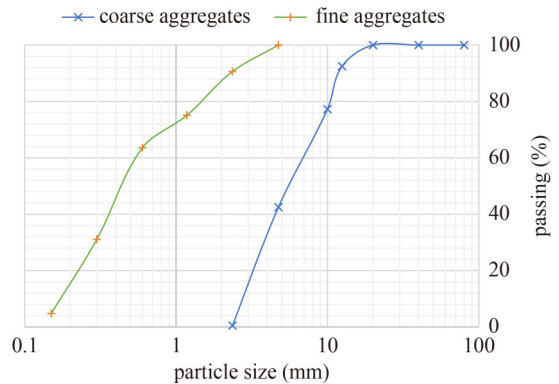In the second step, a NH molarity is selected for the geopolymer mix design, as given in Fig. 3(b), based on the selected Al/binder ratio (0.48) from previous step. The figure contains Al/binder ratios from 0.35 to 0.55 and NH molarities from 8 to 12 mol·L^{-1} on the X and Y axis, respectively. For a 30 MPa target strength, the NH

molarity is selected for mix design (i.e., 10 $mol \cdot L^{-1}$) based on the adopted 0.46 Al/binder ratio and values from Fig. 3(b).

Step 3: NH molarity ($mol \cdot L^{-1}$) vs NS/NH ratio

In the third step, the NS/NH ratio is selected according to Fig. 3(c). Figure 3(c), which contains the NS/NH ratio and NH molarity on the X and Y axis, respectively. The NS/NH ratio is given from 2 to 3, whereas molarity is given from 8 to 12 $mol \cdot L^{-1}$. For example, 10 $mol \cdot L^{-1}$ NH is selected in the previous step using Fig. 3(b) based on the Al/binder ratio. Similarly, a NS/NH ratio of 2.5 will be selected based on the 10 $mol \cdot L^{-1}$ value from the contour plots, as shown in Fig. 3(c).

Step 4: NH molarity ($mol \cdot L^{-1}$) and NS/NH ratio vs water/solid ratio

In the last step, the water/solid ratio is selected based on the NH molarity and NS/NH ratio, which were selected based on the Al/binder ratio and binder content. Figure 3(d) contains the NH molarity ($mol \cdot L^{-1}$) in the X axis from 8 to 12 $mol \cdot L^{-1}$ and water/solid ratio on the Y axis from 0.2 to 0.35. Using the selected 10 $mol \cdot L^{-1}$ molarity and 2.5 NS/NH from the previous steps, a water/solid ratio of 0.250 is selected for the mix design of geopolymer concrete.

Step 5: Calculation of quantities of geopolymer concrete

(a) The selected factors from 2D contour plots of the M30 design mix for ambient curing temperature is given in Table 7.

(b) The physical properties of FA, GGBS, NH, NS, CA, and FS evaluated for mix design calculations are given in Table 8.

(c) The alkali content of the M30 mix was calculated using the binder content and Al/binder ratio. The binder contains 20% GGBS and replaced with FA using a volumetric approach. The total alkali content in geopolymer concrete consists of both NH and NS. The Al/binder ratio of 0.46 results in a total alkali content of 193.2 $kg \cdot m^{-3}$ and their calculations are given below.

$$\frac{\text{Alkali}}{\text{Binder}} = 0.46, \text{ therefore,}$$
$$\text{Alkali content} = 0.46 \times 420 = 193.2 \text{ kg} \cdot m^{-3}$$

(d) The NH and NS contents were calculated using the total alkali content for 10 $mol \cdot L^{-1}$ NH and 2.5 NS/NH ratio. The calculations of NH and NS are given below.

$$\frac{\text{NS}}{\text{NH}} = 2.5, \tag{1}$$

$$\text{NS} + \text{NH} = 193.2 \text{ kg} \cdot m^{-3}. \tag{2}$$

Solving Eq. (1) and (2)

$$\text{NH} = 55.2 \text{ kg} \cdot m^{-3}, \text{ NS} = 138 \text{ kg} \cdot m^{-3}$$

Table 7 Selected factors for mix design of M30 mix

factors	value
curing temperature	ambient temperature (25 °C)
binder content	420 $kg \cdot m^{-3}$
GGBS	20%
Al/binder ratio	0.46
NH molarity	10 M
NS/NH ratio	2.5
water/solid ratio	0.250

Table 8 Physical properties of material used in mix design of geopolymer concrete

property	FA	GGBS	NH	NS	coarse aggregates	fine aggregates
specific gravity	2.2	2.85	1.32	1.53	2.61	2.53
water absorption	–	–	–	–	0.5%	1.5%

(e) After calculating the NH and NS content, additional water (if any) was calculated based on selected water/solid ratio. The water/solid ratio is defined as the total water content of NH, NS, and additional water to the solid content of NH, NS, and total binder content. For 10 $mol \cdot L^{-1}$ NH, it contains 31.4% solid NH pellets 68.6% water. NS contains 44.1% solid content and the remainder as water according to the manufacturer. Furthermore, the total binder content for a M30 mix design was 420 $kg \cdot m^{-3}$. For the selected water/solid ratio of 0.25, the additional water calculations are given below.

For a total NH content of 55.2 $kg \cdot m^{-3}$, the solid content (31.4%) is 17.33 $kg \cdot m^{-3}$ and water content is 37.87 $kg \cdot m^{-3}$. Similarly, for a total NS content of 138 $kg \cdot m^{-3}$, the solid content is 60.85 $kg \cdot m^{-3}$ and water content is 77.14 $kg \cdot m^{-3}$.

$$\frac{\text{water}}{\text{solids}} = \frac{\text{NH (water)} + \text{NS (water)} + \text{additional water (w)}}{\text{NH (solids)} + \text{NS (solids)} + \text{binder content}}. \tag{3}$$

Using Eq. (3), the additional water content is calculated as 9.535 $kg \cdot m^{-3}$.

(f) The quantities of coarse and fine aggregates were calculated using an equivalent volumetric approach according to IS 10262:2019. The fine aggregates used in this study are of Zone III as per IS 383:2016 and coarse aggregates with a maximum size of 12.5 mm were used. The volume of coarse aggregates/total aggregates ratio was calculated based on the selected Al/binder ratio of geopolymer concrete. For a M30 mix and Al/binder ratio of 0.46, the obtained volume of coarse aggregate/total aggregates ratio is 0.558. The quantities of coarse and fine aggregates were calculated using a volumetric approach. A 1% of air content was considered as per IS 10262:2019. The quantities of aggregates were calculated using Eq. (4) given below.

$$0.99 \text{ m}^3 = \frac{Mass(\text{FA})}{S.G.(\text{FA}) \times 1000} + \frac{Mass(\text{GGBS})}{S.G.(\text{FA}) \times 1000}$$
$$+ \frac{Mass(\text{NH})}{S.G.(\text{NH}) \times 1000} + \frac{Mass(\text{NS})}{S.G.(\text{NS}) \times 1000}$$
$$+ \frac{Mass(\text{water})}{S.G.(\text{water}) \times 1000} + \frac{Mass(\text{CA})}{S.G.(\text{CA}) \times 1000}$$
$$+ \frac{Mass(\text{FS})}{S.G.(\text{FS}) \times 1000}. \tag{4}$$

Volume of all in aggregates

$$(V_T) = \frac{Mass(\text{CA})}{S.G.(\text{CA}) \times 1000}$$
$$+ \frac{Mass(\text{FA})}{S.G.(\text{FA}) \times 1000} = 0.6576 \text{ m}^3,$$

$$\text{Mass of CA} = 0.6576 \times 0.558 \times 2.61 \times 1000$$
$$= 957.71 \text{ kg} \cdot \text{m}^{-3},$$

Similarly

$$\text{Mass of FA} = 0.6576 \times 0.442 \times 2.53 \times 1000$$
$$= 735.36 \text{ kg} \cdot \text{m}^{-3}.$$

For ambient curing, 2D contour plots of 50, 60, and 70 MPa target compressive strength are given in Figs. 4(a)–4(d). For heat curing (60 °C), 2D contour plots

of 20, 30, and 40 MPa and 50, 60, and 70 MPa target compressive strength are given in Figs. 5(a)–5(d) and Figs. 6(a)–6(d), respectively. The 2D contour plots for heat curing (90 °C) are given in Figs. 7(a)–7(d) and Figs. 8(a)–8(d).

Similar procedure and calculations of the M30 geopolymer mix for ambient curing, discussed above, is applicable to other target compressive strengths and curing regimes.

4.3 Mix proportioning, mixing, and casting of geopolymer concrete

The input factors of geopolymer concrete, such as binder content, Al/binder ratio, NH-molarity, NS/NH ratio, and water/solid ratio for each curing regime are given in Table 9. The mix proportioning (kg·m^{-3}) are given in Table 10. For geopolymer concrete mixing, the binder was first mixed with coarse and fine aggregates for 5 minutes. Then, the alkali activator solution was poured into dry mix and mixed for another 8–10 min to obtain a consistent mix. Lastly, the fresh geopolymer mix was poured into the molds and sealed with poly wrap to reduce moisture loss. The sealed specimens were cured at room temperature for ambient curing or kept in an oven for 24 hours for heat curing.

Table 9   Mix design input variables selected from different contour graphs

mix	curing regime	total binder content (kg·m^{-3})	GGBS (%)	Al/binder ratio	NH-molarity (mol·L^{-1})	NS/NH ratio	water/solid ratio
M30	ambient	420	20	0.46	10	2.5	0.250
	60	420	0	0.47	10	3	0.255
	90	420	0	0.50	10	3	0.265
M50	ambient	470	30	0.6	12	2	0.275
	60	470	10	0.56	12	2	0.260
	90	470	10	0.58	12	2.2	0.275
M70	ambient	470	40	0.49	14	1.5	0.27
	60	470	30	0.52	14	1.8	0.245
	90	470	20	0.5	14	2	0.250

Table 10   Mix proportioning of geopolymer mixes in kg·m^{-3}

mix	curing temperature	FA	GGBS	NH	NS	additional water	coarse aggregates	fine aggregates
M30	25 °C	336	109	55.2	138	9.535	958	735
	60 °C	420	0	49.35	148	11.09	949	735
	90 °C	420	0	52.5	157.5	10.02	928	736
M50	25 °C	329	183	90.87	181.73	–	791	680
	60 °C	423	61	84.6	169.2	–	822	684
	90 °C	423	61	85.19	187.41	1.24	866	762
M70	25 °C	282	244	92.12	138.18	21.26	831	654
	60 °C	329	183	87.29	157.11	0.92	840	677
	90 °C	376	122	81.47	162.93	4.06	845	670

4.4 Compressive strength test

The compressive strength test was performed for all mixes with a 100 mm × 100 mm × 100 mm cube, as per IS 516 [40], and comparatively used for qualitative analysis. Testing was performed at 7 and 28 d of curing to validate the proposed RSM model. The average results of the three specimens were taken as the final result of the compressive strength for each mix.

5 Results and discussion

5.1 Compressive strength test

The compressive strength of the three mixes with different curing regimes are presented in Figs. 10(a)–10(c). Results show that the compressive strength gets close to the target strength after 28 d of curing for all mixes. For the M30 geopolymer concrete mix at ambient curing, the total binder content was 420 kg·m^{-3} with 80% FA and 20% GGBS. Its compressive strength reaches approximately 71% at 7 d of curing compared to that at 28 d. The addition of GGBS with FA plays a significant role in the increase of compressive strength during the early ages of ambient curing. The geopolymer matrix began to form at 7 d of curing with the dissolution of alkali activators by FA, as shown in Fig. 11(a). At 28 d of curing, the C-S-H gel formed with the geopolymer matrix further increased the strength, as shown in Fig. 11(b). Serag Faried et al. [47] also revealed that, with the help of microstructure, the addition of GGBS aids in C-S-H gel polymerization to achieve the target strength. However, for 60 and 90 °C heat curing of the same mix (0% GGBS), compressive strength reaches approximately 86% at 7 d of curing relative to that at 28 d. Heat curing of the geopolymer mixes help increase the maximum strength during the early stages without the addition of GGBS [13]. At 60 °C heat curing, the geopolymer matrix formed at 7 d of curing. Later at 28 d, the matrix appeared as a fibrous structure in the form of Si-Al bonds, which forms a densify geopolymer concrete microstructure, as shown in Figs. 11(c) and 11(d), respectively. Similarly, for 90 °C heat curing, the geopolymer matrix formed at 7 d of curing and appeared as a densify microstructure at 28 d of curing. The results above show that the addition of calcium rich mineral (GGBS) and temperature both play significant roles in the strength development of geopolymer concrete. Moreover, the variation of other factors, such as Al/binder ratio, NS/NH ratio, and water/solid ratio with different curing regimes also play significant roles in the strength development of geopolymer concrete.

For a M50 geopolymer concrete mix with 30% GGBS at ambient curing, the 7 d strength reaches 63% of the 28 d curing strength. The total binder content used was
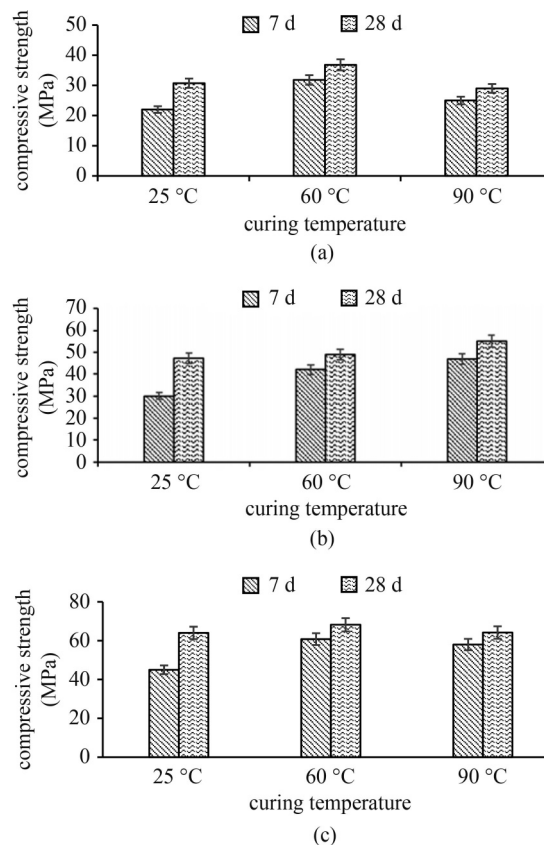

Fig. 10 Measured values of compressive strength at 7 d and 28 d of curing at 25, 60 and 90° C curing for: (a) M30, (b) M50, (c) M70, geopolymer concrete mix.

470 kg·m^{-3} and GGBS content was increased by 10% compared to the M30 mix for ambient curing. Moreover, the Al/binder ratio and NH molarity also increased compared to the M30 mix. The increase in total binder content, GGBS, Al/binder ratio, and molarity helped the specimen achieve the target strength at 28 d of curing. The increase in Al/binder provides sufficient silicates and hydroxides to form the appropriate geopolymer network to attain the target strength. Additionally, the increase in NH molarity helps to dissolve the Si and Al ions, speeding up the geopolymer reaction, forming the density microstructure, and increasing the compressive strength of geopolymer concrete [48]. For 60 °C and 90 °C curing of the same mix, the GGBS content decreased to 10% compared to ambient curing. The compressive strength reached 85% at 7 d of curing compared to that at 28 d of curing for both 60 and 90 °C curing. For the M50 geopolymer concrete mix, variations in GGBS content and water/solid ratio with different curing regimes are the main factors that affect the target strength. Figure 11(e) shows that at 7 d of heat curing, FA was significantly reacted during the initial stage to help attain approximately 85% of the target compressive strength.

For the M70 geopolymer concrete mix at ambient curing, 40% GGBS was blended with FA to attain the
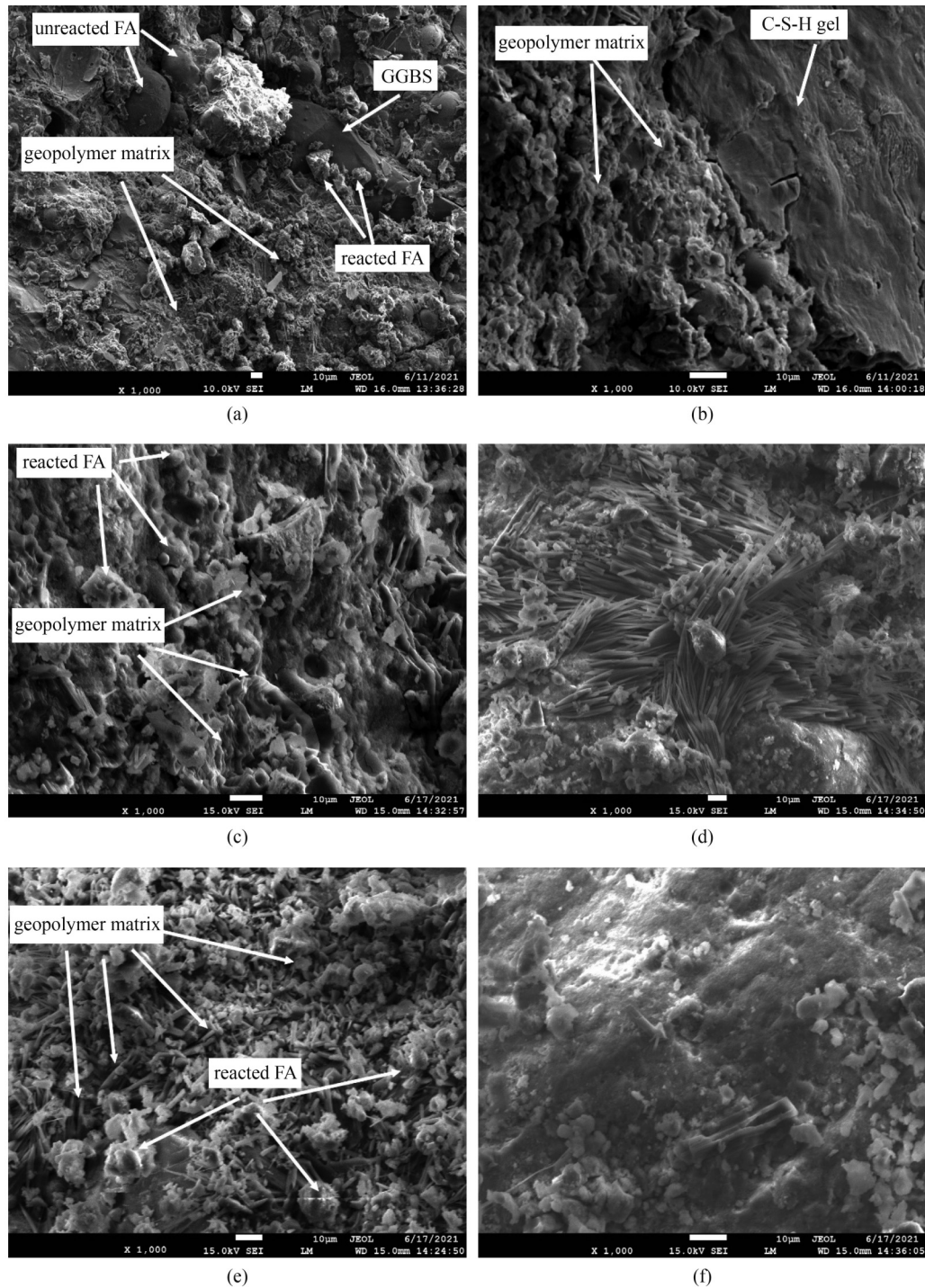
Fig. 11 SEM images showing geopolymer reaction along with GGBS at (a) 7 d and (b) 28 d of ambient curing , formation of geopolymer matrix at (c) 7 d and (d) 28 d of 60° C heat curing, FA reaction (e) 7 d and (f) 28 d of 90° C heat curing

target strength. At 7 d of curing, the compressive strength reached up to 70% of 64 MPa at 28 d, which was about 91% of the target strength. For the M70 mix, the NH molarity increased and NS/NH ratio decreased compared to that of the M30 and M50 geopolymer concrete mixes. The increase in NH content and molarity improved the compressive strength of geopolymer concrete. For the same mix at heat curing, the compressive strength

reached approximately 88% and 90% for 60 and 90 °C, respectively, after 7 d of curing compared to the 28 d compressive strength. The compressive strength reached 97% and 91% of target strength at 28 d of curing for 60 and 90 °C curing, respectively. Figure 11(f) shows the densify microstructure of geopolymer concrete, which helped to attain target compressive strength of the M70 geopolymer concrete. The GGBS content, Al/binder ratio,

NS/NH ratio, and water/solid ratio varies with the different curing regimes for the same mix.

5.2 Stress−strain behavior

The stress−strain behavior and internal behavior of the material help to identify the exact failure pattern during performance evaluation [49,50]. In the current study, stress−strain behavior was observed for all three mixes (M30, M50, and M70) for experimental validation, as shown in Figs. 12(a)–12(i). For the M30 mix at ambient curing, the maximum strain reached 0.003 and 0.0024 at
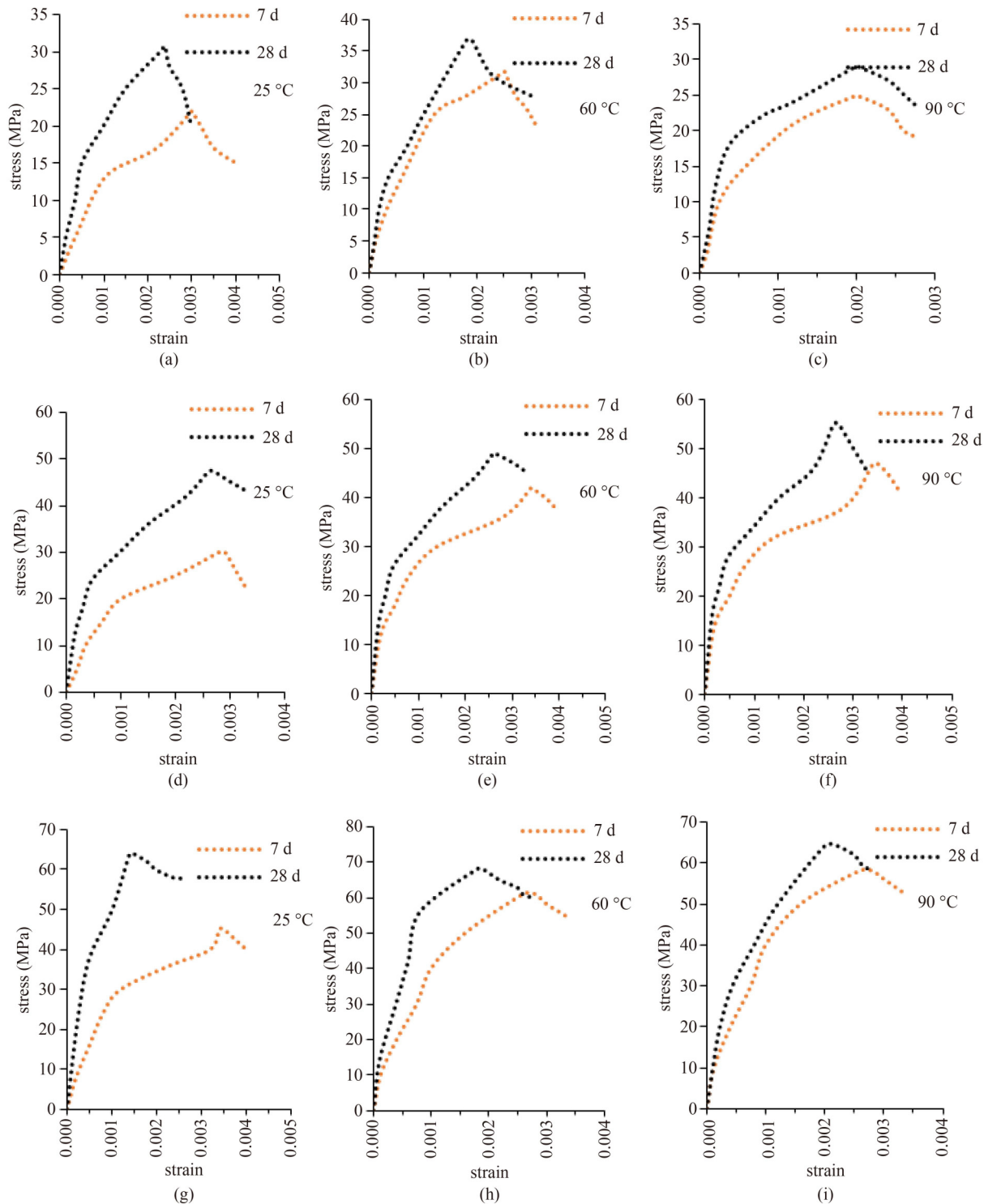

Fig. 12 Stress−strain behavior of mix M30: (a) 25 °C, (b) 60 °C, (c) 90 °C; M50: (d) 25 °C, (e) 60 °C, (f) 90 °C; M70: (g) 25 °C, (h) 60 °C, (i) 90 °C at different curing regime.

7 and 28 d of curing, respectively, as shown in Fig. 12(a). The stress−strain curve at 7 d of curing with 60 and 90 °C heat curing was steeper than ambient curing curve since the compressive strength reached nearly 86% of the 28 d strength, as discussed above. Albidah et al. [51] also investigated the stress−strain behavior of geopolymer concrete at elevated temperatures and found that it demonstrates a steeper curve at high temperatures. At 28 d of curing, the maximum strain reached 0.0020 for both 60 and 90 °C heat curing, as shown in Figs. 12(b) and 12(c). For the M50 mix, the peak stress increased as the compressive strength increased due to the lower NS/NH ratio, higher molarity, and higher GGBS content. Verma and Dev [9] showed that increasing the NH molarity results in lower strain values and higher modulus of elasticity. Previous studies also show that an increase in GGBS content densifies the geopolymer concrete and reduces the strain value to achieve a higher compressive strength [52,53]. At ambient curing, the maximum strain reaches 0.0029 and 0.0027 at 7 and 28 d of curing, respectively, as shown in Fig. 12(d). For 60 and 90 °C heat curing, the M50 mix demonstrated a similar trend as the M30 mix, i.e., a stress−strain curve with a steeper slope at 7 d of curing, as shown in Figs. 12(e) and 12(f). For the M70 mix, the stress−strain peak became steeper during all stages of curing due to the increase in both NH molarity and GGBS content, as seen in Figs. 12(g)–12(i). The overall results show that heat cured geopolymer concrete demonstrate lower strain at both 7 and 28 d of curing, resulting in stiffer and denser geopolymer concrete under heat curing conditions than ambient curing. Moreover, the decrease in NS/NH ratio, as well as increase in GGBS content and NH molarity also result in lower strain values at higher compressive strengths.

5.3   Relation between experimental and predicted compressive strength

The experimental and predicted compressive strengths after 28 d of curing with different curing regimes are shown in Fig. 13. Results show that the experimental values of compressive strength and predicted values from the RSM model demonstrate good fit with a R^2 value of
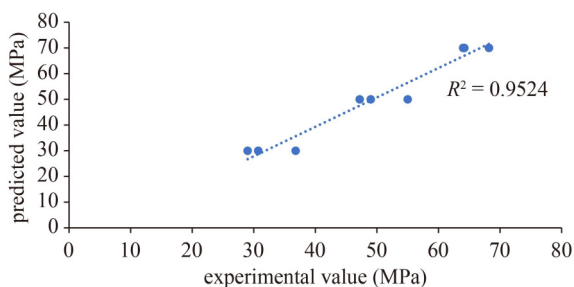

Fig. 13   Relation between experimental and predicted value of compressive strength at 28 d of curing at all curing regime.

0.95. The M30 mix showed compressive strengths of 30.72, 36.8, and 29 MPa after 28 d at 25, 60, and 90 °C curing, respectively, in comparison to the predicted value of 30 MPa. Similarly, for the M50 mix, the observed compressive strengths after 28 d were 47.2, 49, and 55 MPa at 25, 60, and 90 °C curing, respectively. The M70 mix also showed similar results to the predicted value with all curing regimes.

6   Effect of input factors on compressive strength

6.1   Coefficient estimates from coded equation

The compressive strengths of the M30, M50, and M70 mixes were validated through 2D contour plots of different input factors and the experimental compressive strength values show good fit with that predicted by the RSM model. Each input factor individually affects the compressive strength and the coded equation for compressive strength based on selected RSM quadratic model is given below.

$$\begin{aligned}
\text{Compressive Strength} = {} & 51.92 - 5.05A + 10.70B \\
& + 30.06C - 63.28D + 3.10E - 50.86F \\
& + 9.57G - 46.61AC - 14.30AD \\
& - 15.75AE + 32.17AF + 26.76BC \\
& - 50.17BD - 4.72BG + 63.19CE \\
& - 57.89DF - 59.78EF + 3.96B^2 \\
& - 20.83C^2 - 9.19D^2 - 5.66G^2.
\end{aligned}$$

(A: binder content, B: GGBS%, C: Al/binder, D: NS/NH, E: NH molarity, F: water/solids, G: temperature)

The equation in terms of the coded factors is used to predict the output variable compressive strength. The coded equation is useful for identifying the relative impact of each factor by comparing the factor coefficients, known as coefficient estimates. The coefficient estimates and standard errors of the coded equation are presented in Table 11. The coefficient estimate represents the expected change, in response, per unit change, in factor value, when all remaining factors are held constant. The intercept in an orthogonal design is the overall average response of all the runs.

The coefficient estimates of the input parameters are shown in Fig. 14. The coefficient estimates of −5.05 of input factor A (Binder content) suggests that it has the least effect on the compressive strength of geopolymer concrete, in other words, solely changing the binder content will not affect the compressive strength significantly. The coefficient estimates of 10.70 of input factor B (GGBS%) shows that increasing the GGBS content will likely increase the compressive strength.

However, input factors C (Al/binder) and D (NS/NH) have significant effects on the compressive strength of geopolymer concrete. Increasing the binder content will increase the compressive strength, whereas increasing the NS/NH value will decrease the compressive strength. For the M30 mix, the selected NS/NH range was 2.5 to 3, whereas for the M50 and M70 mixes, the ranges were 2

to 2.5 and 1.5 to 2, respectively. The coefficient estimate value of −50.86 for input factor F (water/solids) shows that it has a significant effect on compressive strength, specifically, increasing the water/solid ratio will decrease the compressive strength of geopolymer concrete. The 9.57 coefficient estimate of input factor G (temperature) shows that increasing the temperature will also increase the compressive strength. Overall, results show that input factors C (Al/binder), D (NS/NH), and F (water/solids) have significant effects on compressive strength. However, input factors A (binder content), B (GGBS%), and E (NH molarity) are individually less impactful on compressive strength.

Table 11 Coefficient estimates and standard error of input variables in form of coded factors

factor	coefficient estimate	standard error
intercept	51.92	2.7
A	−5.05	3.56
B	10.7	1.69
C	30.06	5.66
D	−63.28	8.16
E	3.11	2.77
F	−50.87	3.28
G	9.58	1.92
AC	−46.61	5.64
AD	−14.3	5.49
AE	−15.75	3.81
AF	32.17	6.33
BC	26.77	4.61
BD	−50.18	7.1
BG	−4.73	2.21
CE	63.2	6.1
DF	−57.9	8.78
EF	−59.78	4.57
B^2	3.97	1.94
C^2	−20.84	6.29
D^2	−9.2	3.79
G^2	−5.66	2.35

6.2 Variation of input factor with respect to compressive strength

The variation of each input factor with respect to compressive strength are shown in Figs. 15(a)–15(g), which were evaluated based on the average value of input factors tabulated in Table 1. Figure 15(a) shows that increasing the binder content will not affect the compressive strength significantly. An increase in the GGBS content of geopolymer concrete tends to increase the compressive strength linearly, as shown in Fig. 15(b). The GGBS content was varied in the RSM model with respect to the target compressive strength and curing regime. The Al/binder ratio shows a nonlinear effect on compressive strength, where an increase in Al/binder ratio will first increase then decrease the compressive strength, as seen from Fig. 15(c). Figure 15(d) shows that the NS/NH ratio plays a significant role, specifically, increasing the NS/NH ratio will linearly decrease compressive strength. However, the effect of NH molarity on compressive strength in lesser than NS/NH ratio and Al/binder ratio as shown in Fig. 15(e). The water/solid ratio showed a decreasing trend in compressive strength as their values increased. Figure 15(f) shows that the water/solid ratio also plays an
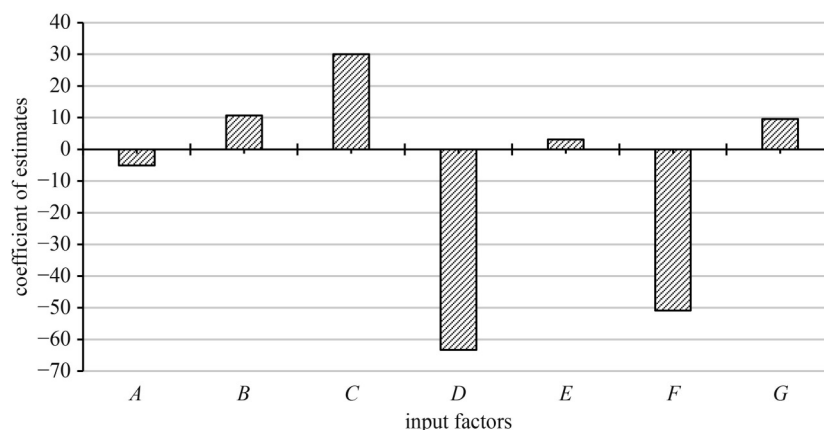

Fig. 14 Coefficient estimate of input factors based on coded equation of compressive strength. A: binder content, B: GGBS%, C: Al/binder, D: NS/NH, E: NH molarity, F: water/solids, G: temperature.
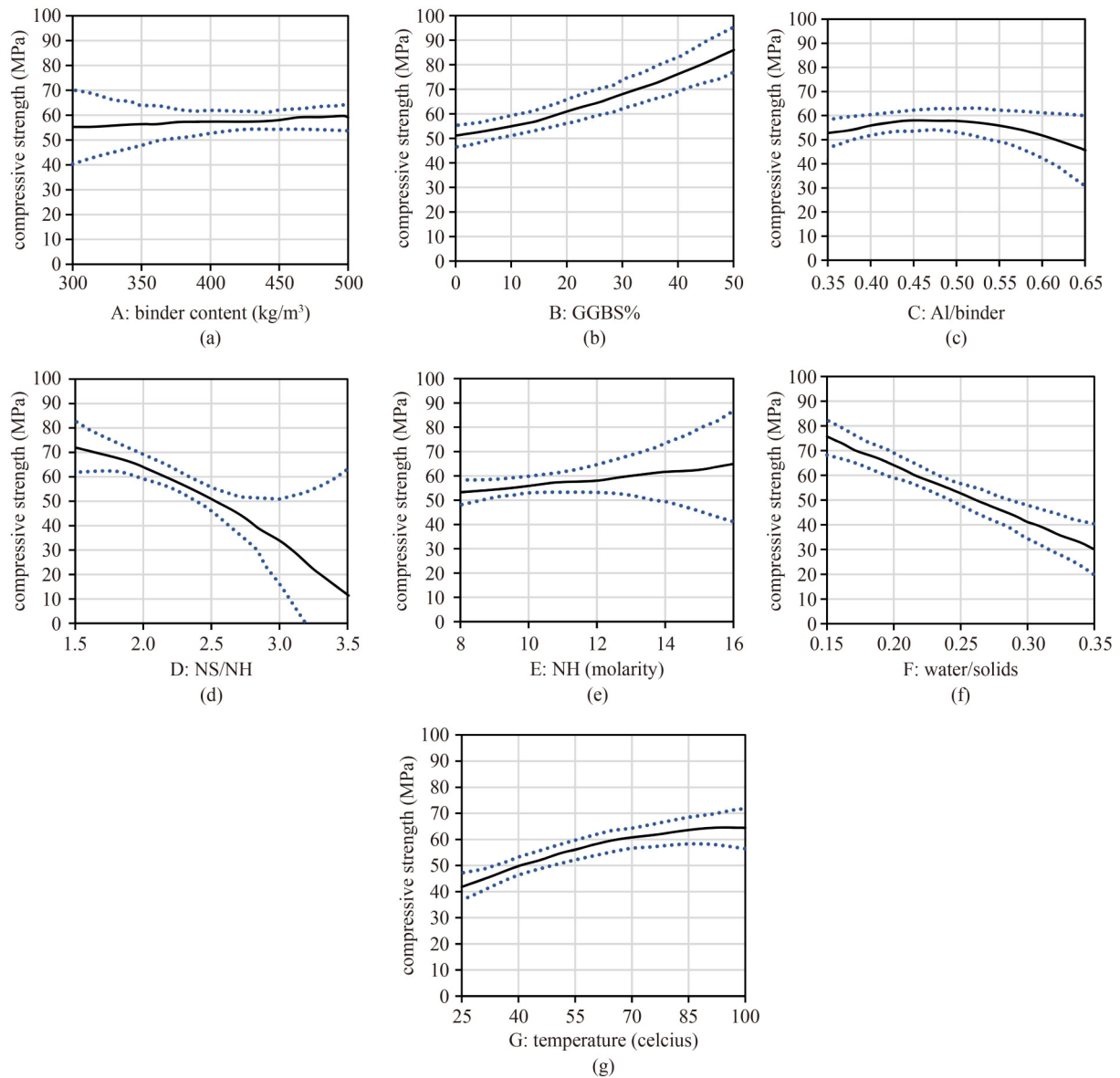
Fig. 15   Variation of input factors with respect to compressive strength for mix design method of geopolymer concrete.

important role in the output value of compressive strength, similar to the NS/NH ratio. Figure 15(g) illustrates the relation between temperature and compressive strength and that temperature will first increase then decrease the compressive strength past a certain point. However, the adopted RSM model categorized temperature into three levels, i.e., one ambient curing (25 °C) and two heat curing (60 and 90 °C). The overall results from varying each input factor revealed that the NS/NH ratio, water/solid ratio, and Al/binder ratio (decreasing order of significance) play significant roles on compressive strength.

7   Conclusions

The mix design method of geopolymer concrete was proposed based on the literature database obtained using RSM. The 2D contour plots of different factors with different curing regimes for all three mixes from the proposed model were validated through experimentation.

1) The RSM quadratic model used in this study for the mix design demonstrated good fit for multiple factors with a significant p-value of less than 0.05. Furthermore, the adjusted R^2 value of 0.85 shows good relation between the different factors used for the mix design of geopolymer concrete.

2) The three mixes (i.e., M30, M50, and M70) used for model validation showed promising results at 28 d for all curing regimes. At 7 d of ambient curing, the strength reached 60%–70% of their target strength. For heat curing at 60 and 90 °C, compressive strength reached 85%–90% of their target strength at 7 d of curing. The compressive strength at 28 d of all three mixes was over

90% of their target strength for all curing regimes.

3) The experimental and predicted values from the RSM model showed good relation with a R^2 value of 0.95. Moreover, the coefficient estimate of the RSM model with respect to the experimental results shows that the NS/NH ratio, water/solid ratio, and Al/binder ratio (decreasing order of significance) play significant roles on the compressive strength of geopolymer concrete. The binder content demonstrated the least effect on compressive strength.

References

1. Rashad A M, Sadek D M, Hassan H A. An investigation on blast-furnace stag as fine aggregate in alkali-activated slag mortars subjected to elevated temperatures. Journal of Cleaner Production, 2016, 112: 1086−1096

2. Ali M B, Saidur R, Hossain M S. A review on emission analysis in cement industries. Renewable and Sustainable Energy Reviews, 2011, 15: 2252−2261

3. Davidovits J. Geopolymer Institute Library. Technical Paper #24, False-CO_2-Values. Saint-Quentin: Geopolymer institute library, 2015

4. Gunasekara C, Law D W, Setunge S. Long term permeation properties of different fly ash geopolymer concretes. Construction & Building Materials, 2016, 124: 352−362

5. Kong D L Y, Sanjayan J G, Sagoe-Crentsil K. Factors affecting the performance of metakaolin geopolymers exposed to elevated temperatures. Journal of Materials Science, 2008, 43(3): 824−831

6. Davidovits J. Geopolymers. Journal of Thermal Analysis, 1991, 37(8): 1633−1656

7. Bernal S A, Mejía De Gutiérrez R, Pedraza A L, Provis J L, Rodriguez E D, Delvasto S. Effect of binder content on the performance of alkali-activated slag concretes. Cement and Concrete Research, 2011, 41(1): 1−8

8. Hardjito D, Wallah S E, Sumajouw D M J, Rangan B. V: Fly ash-based geopolymer concrete. Australian Journal of Structrural Engineering, 2005, 6(1): 77−86

9. Verma M, Dev N. Sodium hydroxide effect on the mechanical properties of flyash-slag based geopolymer concrete. Structural Concrete, 2021, 22(S1): E368−E379

10. Noushini A, Castel A. The effect of heat-curing on transport properties of low-calcium fly ash-based geopolymer concrete. Construction & Building Materials, 2016, 112: 464−477

11. Hassan A, Arif M, Shariq M. Effect of curing condition on the mechanical properties of fly ash-based geopolymer concrete. SN Applied Sciences, 2019, 1(12): 1694

12. Kong D L Y, Sanjayan J G. Effect of elevated temperatures on geopolymer paste, mortar and concrete. Cement and Concrete Research, 2010, 40(2): 334−339

13. Mallikarjuna Rao G, Gunneswara Rao T D. A quantitative method of approach in designing the mix proportions of fly ash and GGBS-based geopolymer concrete. Australian Journal of Civil Engineering, 2018, 16(1): 53−63

14. Nath P, Sarker P K. Effect of GGBFS on setting, workability and early strength properties of fly ash geopolymer concrete cured in ambient condition. Construction & Building Materials, 2014, 66: 163−171

15. Nagajothi S, Elavenil S. Effect of GGBS addition on reactivity and microstructure properties of ambient cured fly ash based geopolymer concrete. Silicon, 2021, 13: 507−516

16. Li N, Shi C, Zhang Z, Zhu D, Hwang H J, Zhu Y, Sun T. A mixture proportioning method for the development of performance-based alkali-activated slag-based concrete. Cement and Concrete Composites, 2018, 93: 163−174

17. Pavithra P, Srinivasula Reddy M, Dinakar P, Hanumantha Rao B, Satpathy B K, Mohanty A N. A mix design procedure for geopolymer concrete with fly ash. Journal of Cleaner Production, 2016, 133: 117−125

18. Patankar S V, Ghugal Y M, Jamkar S S. Mix design of fly ash based geopolymer concrete. In: Proceeding of Advances in Structural Engineering: Materials, Volume Three. Springer New Delhi, 2015, 1619−1634

19. Ferdous M W, Kayali O, Khennane A. A detailed procedure of mix design for fly ash based geopolymer concrete. In: Proceedings of the Fourth Asia-Pacific Conference on FRP in Structures (APFIS 2013). Melbourne: International Institute for FRP in Construction, 2013

20. Anuradha R, Sreevidya V, Venkatasubramani R, Rangan B V. Modified guidelines for geopolymer concrete mix design using indian standard. Asian Journal of Civil Engineering, 2012, 13: 357−368

21. Talha Junaid M, Kayali O, Khennane A, Black J. A mix design procedure for low calcium alkali activated fly ash-based concretes. Construction & Building Materials, 2015, 79: 301−310

22. Luan C, Shi X, Zhang K, Utashev N, Yang F, Dai J, Wang Q. A mix design method of fly ash geopolymer concrete based on factors analysis. Construction & Building Materials, 2021, 272: 121612

23. Bondar D, Ma Q, Soutsos M, Basheer M, Provis J L, Nanukuttan S. Alkali activated slag concretes designed for a desired slump, strength and chloride diffusivity. Construction & Building Materials, 2018, 190: 191−199

24. Hadi M N S, Farhan N A, Sheikh M N. Design of geopolymer concrete with GGBFS at ambient curing condition using Taguchi method. Construction & Building Materials, 2017, 140: 424−431

25. Karthik S, Saravana K, Mohan R. A Taguchi approach for optimizing design mixture of geopolymer concrete incorporating fly ash. Ground Granulated Blast Furnace Slag and Silica Fume, Crystals, 2021, 11: 1079

26. Riahi S, Nazari A, Zaarei D, Khalaj G, Bohlooli H, Kaykha M M. Compressive strength of ash-based geopolymers at early ages designed by Taguchi method. Materials & Design, 2012, 37: 443−449

27. Olivia M, Nikraz H. Properties of fly ash geopolymer concrete designed by Taguchi method. Materials & Design, 2012, 36: 191−198

28. Lokuge W, Wilson A, Gunasekara C, Law D W, Setunge S. Design of fly ash geopolymer concrete mix proportions using Multivariate Adaptive Regression Spline model. Construction & Building Materials, 2018, 166: 472−481

29. Gunasekara C, Atzarakis P, Lokuge W, Law D W, Setunge S. Novel analytical method for mix design and performance prediction of high calcium fly ash geopolymer concrete. Polymers, 2021, 13(6): 900

30. Vu-Bac N, Lahmer T, Keitel H, Zhao J, Zhuang X, Rabczuk T. Stochastic predictions of bulk properties of amorphous polyethylene based on molecular dynamics simulations. Mechanics of Materials, 2014, 68: 70−84

31. Vu-Bac N, Lahmer T, Zhang Y, Zhuang X, Rabczuk T. Stochastic predictions of interfacial characteristic of polymeric nanocomposites (PNCs). Composites. Part B, Engineering, 2014, 59: 80−95

32. Vu-Bac N, Lahmer T, Zhuang X, Nguyen-Thoi T, Rabczuk T. A software framework for probabilistic sensitivity analysis for computationally expensive models. Advances in Engineering Software, 2016, 100: 19−31

33. Vu-Bac N, Silani M, Lahmer T, Zhuang X, Rabczuk T. A unified framework for stochastic predictions of mechanical properties of polymeric nanocomposites. Computational Materials Science, 2015, 96: 520−535

34. Hamdia K M, Silani M, Zhuang X, He P, Rabczuk T. Stochastic analysis of the fracture toughness of polymeric nanoparticle composites using polynomial chaos expansions. International Journal of Fracture, 2017, 206(2): 215−227

35. Vu-Bac N, Rafiee R, Zhuang X, Lahmer T, Rabczuk T. Uncertainty quantification for multiscale modeling of polymer nanocomposites with correlated parameters. Composites. Part B, Engineering, 2015, 68: 446−464

36. Box G E P, Wilson K B. On the experimental attainment of optimum conditions. Journal of the Royal Statistical Society. Series B. Methodological, 1951, 13(1): 1−38

37. Myers R H, Montgomery D C, Anderson-Cook C M. Response Surface Methodology: Process and Product Optimization Using Designed Experiments. New Jersey: Wiley, 2016

38. Habibi A, Ramezanianpour A M, Mahdikhani M, Bamshad O. RSM-based evaluation of mechanical and durability properties of recycled aggregate concrete containing GGBFS and silica fume. Construction & Building Materials, 2021, 270: 121431

39. Koç, B., and F. Kaymak-Ertekin. Response surface methodology and food processing applications. GIDA—Journal of Food, 2010, 35: 63−70

40. Aydar A Y, Bagdatlioglu N, Köseoglu O. Effect of ultrasound on olive oil extraction and optimization of ultrasound-assisted extraction of extra virgin olive oil by response surface methodology (RSM). Grasas y Aceites, 2017, 68(2): 189

41. Andreson M. Stat-Ease. v11. Adequate Precision. Sate Ease Inc. Available at the website of Stat-Ease

42. Deb P S, Nath P, Sarker P K. The effects of ground granulated blast-furnace slag blending with fly ash and activator content on the workability and strength properties of geopolymer concrete cured at ambient temperature. Materials & Design, 2014, 62: 32−39

43. Xie Z, Xi Y. Hardening mechanisms of an alkaline-activated class F fly ash. Cement and Concrete Research, 2001, 31(9): 1245−1249

44. IS. 10262-2019: Concrete Mix Proportioning—Guidelines. New Delhi: Indian Stand, 2019

45. IS. 3812: Specification for Pulverized fuel ash. Part-1: For Use as Pozzolana in Cement, Cement Mortar and Concrete. New Delhi: Indian Stand, 2013, 1−12

46. IS: 383: Specification for Coarse and Fine Aggreagtes from Natural Sources for Concrete. New Delhi: Indian Stand, 2002

47. Serag Faried A, Sofi W H, Taha A Z, El-Yamani M A, Tawfik T A. Mix design proposed for geopolymer concrete mixtures based on ground granulated blast furnace slag. Australian Journal of Civil Engineering, 2020, 18(2): 205−218

48. Somna K, Jaturapitakkul C, Kajitvichyanukul P, Chindaprasirt P. NaOH-activated ground fly ash geopolymer cured at ambient temperature. Fuel, 2011, 90(6): 2118−2124

49. Rabczuk T, Belytschko T. A three-dimensional large deformation meshfree method for arbitrary evolving cracks. Computer Methods in Applied Mechanics and Engineering, 2007, 196(29−30): 2777−2799

50. Rabczuk T, Belytschko T. Cracking particles: A simplified meshfree method for arbitrary evolving cracks. International Journal for Numerical Methods in Engineering, 2004, 61(13): 2316−2343

51. Albidah A, Alqarni A S, Abbas H, Almusallam T, Al-Salloum Y. Behavior of Metakaolin-Based geopolymer concrete at ambient and elevated temperatures. Construction & Building Materials, 2022, 317: 125910

52. Noushini A, Aslani F, Castel A, Gilbert R I, Uy B, Foster S. Compressive stress−strain model for low-calcium fly ash-based geopolymer and heat-cured Portland cement concrete. Cement and Concrete Composites, 2016, 73: 136−146

53. Xie J, Wang J, Rao R, Wang C, Fang C. Effects of combined usage of GGBS and fly ash on workability and mechanical properties of alkali activated geopolymer concrete with recycled aggregate. Composites Part B: Engineering, 2019, 164: 179−190